

Investigation on the High Vacuum Tribological Characteristics of Surface Treated Nuclear Grade Stainless Steel Type AISI 316 LN at 25 to 500 °C

Ayyannan Devaraju^{1,*} – Ayyasamy Elayaperumal¹ – Srinivasan Venugopal² –
Satish V. Kailas³ – Joseph Alphonsa⁴

¹Department of Mechanical Engineering, Engineering Design Division,
College of Engineering, Anna University, India

²Metallurgy and Materials Group, Indira Gandhi Centre for Atomic Research, India

³Department of Mechanical Engineering, Indian Institute of Science, India

⁴Facilitation Centre for Industrial Plasma Technologies, Institute for Plasma Research, India

Although some researchers have published friction and wear data of Plasma Nitride (PN) coatings, the tribological behavior of PN/PN Pairs in high vacuum environment has not been published so far. In order to bridge this knowledge gap, tribological tests under dry conditions have been conducted on PN/PN Pairs for varying temperatures of 25, 200, 400 and 500 °C in high vacuum (1.6×10^{-4} bar) environment. The PN coatings showed good wear resistance layer on the ring surface. The PN coatings were removed only from the pin surface for all the tests since it contacts at a point. The friction and wear were low at lower temperatures and it eliminated adhesion between the contact surfaces until the coating was completely removed from the pin surface.

©2011 Journal of Mechanical Engineering. All rights reserved.

Keywords: nuclear materials, surface treatment, PN layer, elevated temperature, high vacuum, tribological characteristics

0 INTRODUCTION

Austenitic stainless steels exhibit good results in corrosion, vacuum, CO₂ and argon environments [1]. However, this material is restricted to be used directly due to its low surface hardness, high friction and strong adhesion when it is sliding against itself and other metals. Hence, it is to be coated to reduce or eliminate these problems. Among many surface modification techniques, plasma nitriding is the most successfully and widely employed surface treatment to coat the austenitic stainless steels at different temperatures, durations and gas mixtures. It is well known that plasma nitriding offers many advantages over traditional gas nitriding and salt bath nitriding, particularly in terms of reduced gas consumption, reduced energy consumption and the removal of environmental hazards [2] to [7]. In plasma nitriding process, the sputter cleaning effectively removes the oxide film (Cr₂O₃) from the stainless steel surface and thus accelerate the nitrogen mass transfer [4]. Hence, plasma nitriding has been selected for the current study.

In general, when the metals are in sliding contact under high vacuum environment, they exhibit tribological problems of high friction, stick-slip motion and high wear due to strong adhesion between the contact surfaces. In high vacuum environment, metals will become atomically clean due to the absence of oxygen or oxide layer and moisture which usually separates the sliding surfaces and act as lubricants thereby reducing friction and wear [8] and [9]. Only few researchers have done the dry wear tests at elevated temperatures on plasma nitride (PN) coatings [10] and [11]. They have reported that the wear rate was reduced at elevated temperature due to the formation of oxide layer. The ceramic coating loses its hardness and shear strength at elevated temperature [12] and [13]. These studies are useful to know the tribological behaviors of nitride coatings in air environment. However, the wear behavior of plasma nitrided stainless steel in high vacuum environment has not been studied so far. Furthermore, the Prototype Fast Breeder Reactor (PFBR) which under construction at Kalpakkam, India, austenitic Stainless Steel type

*Corr. Author's Address: Department of Mechanical Engineering, Engineering Design Division,
College of Engineering, Anna University, Chennai-600 025, India, adevaa2008@rediffmail.com

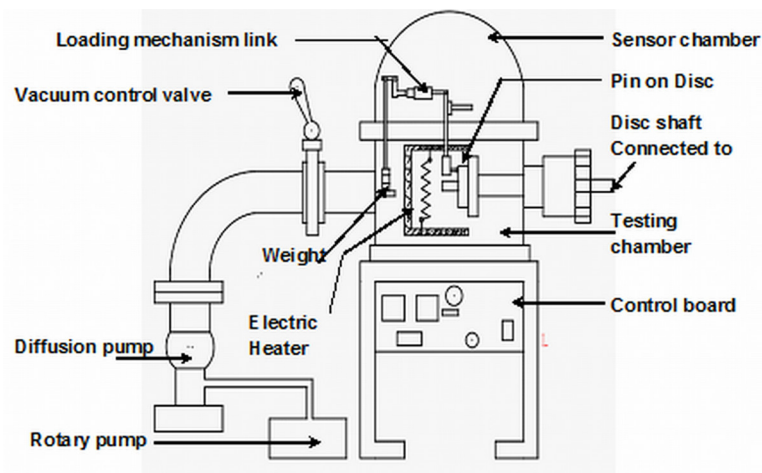


Fig. 1. Schematic view of the vacuum based high temperature Pin-On-Disc machine

AISI 316 LN (316LN SS) is the main structural material with liquid sodium is being used as the coolant for transferring the heat from the reactor to the steam generators [14]. In PFBR, the many important components are sliding at the temperatures of 25 to 500 °C in a high vacuum environment. To simulate its condition, the wear tests were conducted in an equally matching environment. Therefore, in this work 316LN SS was plasma nitrided and its high vacuum tribological characteristics have been evaluated.

1 VACUUM BASED PIN-ON-DISC (VPOD) TRIBOMETER

The schematic view of VPOD tribometer is shown in Fig. 1. The important parts of VPOD tribometer are the testing chamber, the sensor chamber, the disc rotating mechanism, the heating system, loading mechanism, the vacuum built up circuit, the control board and the data measurement system. The testing chamber is a hollow cylindrical shell of diameter 0.45 m and height of 0.35 m. Its base has been closed with a flat stainless steel circular plate. The top has been covered by hemi-spherical shell called sensor chamber. The cylindrical and hemispherical shells are double walled structure. There is a gap in the double walled structure and through this gap, the water is circulated to maintain the structure at room temperature. The testing chamber has been vacuum sealed for all the openings in which

high temperatures and high vacuum experiments are conducted. The rectangular hinged door (not shown in the diagram) has been fitted in front of the testing chamber for loading and unloading of specimens. An 'eye piece' has been fixed in the hinged door to observe the sliding interface between the pin and the disc during the experiments. The disc has been mounted on a horizontal shaft, which was connected to the a d.c servomotor through a timer-belt which avoids the slipping between the belt and pulley. The servomotor provides constant speed with plus or minus one revolution.

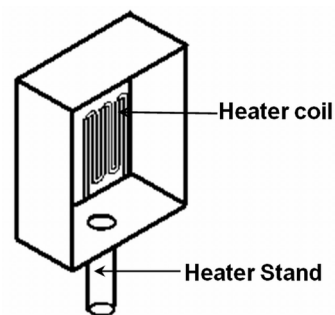


Fig. 2. Schematic view of the heater

An electric resistance heater is used to obtain the different temperatures upto 600 °C. It has been placed in a box cover, so that the heat generated is completely directed to the area where the pin and disc are positioned (Fig. 2). The Proportional Integral Derivative (PID)

controller has been used to maintain the steady temperatures with ± 5 °C. The stationary pin is loaded horizontally against a vertically rotating disc as shown in Fig. 3, which is different from the conventional pin on disc tribometer where the rotating disc was mounted in the horizontal position [15]. The main feature of the VPOD is that it eliminates or reduces the trapping wear debris in the wear track (i.e., third body effect), which alters the wear rate and mechanism. The rotary and diffusion pumps have been connected in a series to the left side of the testing chamber. The initial vacuum is obtained using a rotary pump and the high vacuum (up to 10^{-5} bar) is maintained by the diffusion pump. A penny gauge is used to measure the pressure up to 0.001 bar and a pirani gauge is used to measure the pressure greater than 0.001 bar. The sensor chamber consists of load cell, Linear Voltage Displacement Transducer (LVDT) and the loading lever mechanism. When the dead weight is added in the normal load arm, the loading lever mechanism magnifies one and a half times, approximately. The load cell is capable of measuring loads from 1 to 2000 N. The linear movement of the pin towards the disc can be measured using LVDT with ± 1 micron accuracy. The control board contains the pressure indicator, the temperature indicator, the eater switch and Vacuum pump switch. All the data from the VPOD is acquired using a personal computer. The machine has been fixed on an anti-vibration stand.

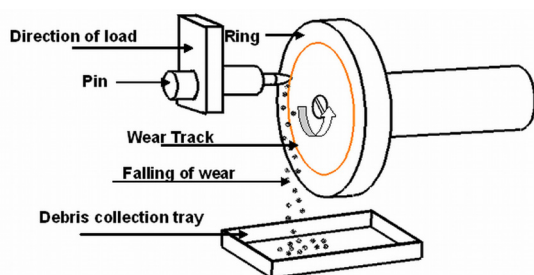


Fig. 3. Schematic diagram of loading configuration of VPOD

2 EXPERIMENTAL METHODS

2.1 Specimen

The 316LN SS was used as the substrate material in this study and its composition was in

wt. % C: 0.02, Ni: 12.1, Cr: 17.9, Si: 0.3, N: 0.07, Mn: 1.8, Mo: 2.4 and Fe: Balance. In order to reduce the material cost and difficulties involved during the post examination works, the discs have been prepared in the form of rings. The 316LN SS was cut from a plate and then machined to the ring geometry of 92 mm outer diameter, 72 mm inner with 1.05 mm radius at one end were tested. The samples were ground using various ranges of the Silicon carbide emery paper and then a mirror polished using diamond paste to obtain the roughness (R_a) of 0.04 μm . The pins and rings were plasma nitrided at 570 °C for 24 hr in a gas mixture of 20% N_2 to 80% H_2 to obtain thicker PN layer under a working pressure of 5 mbar.

2.2 The Microstructure, Microhardness and XRD Test

The cross sectional microstructure of the PN coated surface is examined in a Scanning Electron Microscope (SEM) and its phases were identified by the X - ray Diffraction (XRD) test. It is to be noted that the XRD spectrum was taken in the powder mode with Cu K alpha target and Ni filter. The hardness of the PN coatings was measured by using a Vickers microhardness tester at 25 g load.

2.3 Dry Wear Test

The dry sliding wear tests were conducted on the PN coated ring against PN coated pin at 25, 200, 400 and 500 °C to evaluate the tribological characteristics of PN coatings using VPOD tribometer. All the tests were conducted at the constant sliding speed (0.0576 ms^{-1}), sliding distance (103 m) and normal load (4.1 N) in high vacuum (1.6×10^{-4} bar) environment. The initial Hertzian contact pressure was found to be 2 GPa for the load of 4.1 N. Two or three experiments have been conducted for each condition for the reasonable reproducibility of the results. Prior to wear testing, the rings and pins were cleaned using acetone and then dried for 15 minutes. The electronic balancing machine with the accuracy of 0.00001 g was used to record the mass of material loss during wear tests. The morphology of worn surfaces of pins and rings were examined by SEM.

The 2D optical profilometer was used to measure the depth of the wear track.

3 RESULTS AND DISCUSSION

3.1 The Microstructure, Microhardness and XRD Results

A cross sectional SEM micrograph of plasma nitrided 316LN SS sample is shown in Fig. 4. It reveals that the average thickness of the PN coating layer was 70 μm . The maximum coating thickness was 90 μm near to the edge. The microhardness was measured along the depth on the cross sectional plasma nitrided 316LN SS sample and presented in Fig. 5. The surface hardness was 1040 $\text{HV}_{25\text{g}}$ which is five times higher than the hardness of substrate material (210 $\text{HV}_{25\text{g}}$). In a certain depth (65 to 75 μm) below the nitrided surface, microhardness is reduced gradually and reached to substrate hardness at 300 μm . It is due to the nitrogen diffusion layer. The XRD analysis on the PN coating was performed over the 2θ range from 35 to 90°. The results of the XRD analysis carried on the PN surface (i.e., after the plasma nitriding process) are presented in Fig. 6. They reveal that the PN layer consists of CrN, Fe_4N and Fe_3N phases, in addition to the observation of the austenite reflections from the substrate material.

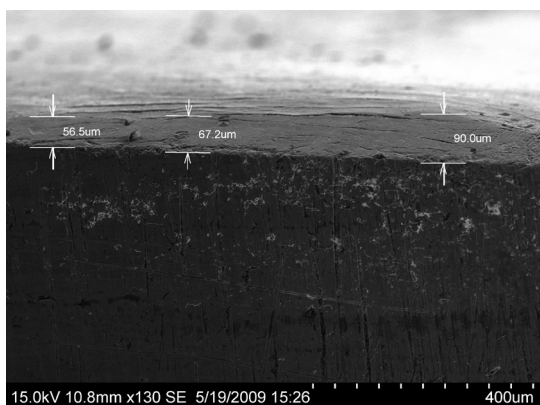


Fig. 4. The cross sectional SEM micrograph of plasma nitrided 316LN SS sample

3.2 The Tribological Test on PN/PN Pair at 25 °C

The PN coated ring– PN coated pin wear test was conducted for one hour for the sliding speed of 0.0576 ms^{-1} , load of 4.1 N and at 25 °C. The variation of coefficient of friction (COF) as a function of the sliding distance is presented in Fig. 7. At 25 °C, the COF was 0.6 up to the sliding distance of 25 m and then, it increased continuously till 82 m sliding distance and it maintains steady at 1.8 (Fig. 7). The PN coated pin slides on the PN coated ring without the coating failure up to 25 m sliding distance. The pin coating started to fail at 25 m. This could be the reason for lower friction to the sliding distance of 25 m.

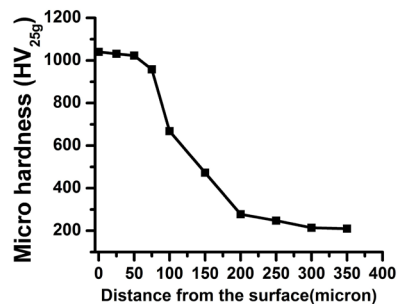


Fig. 5. Microhardness profiles of Plasma nitrided 316LN SS sample

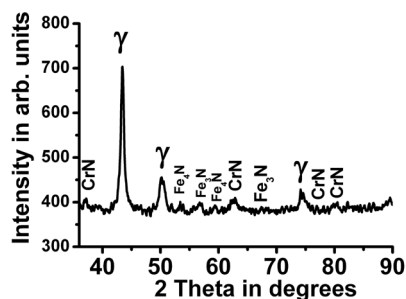


Fig. 6. The XRD patterns of Plasma nitrided 316LN SS sample

When the sliding distance increased beyond 25 m, the real area of contact increased and the coating started to get removed from the pin surface. Therefore, instead of PN/PN contact, it became partly 316LN/PN in addition to PN/PN between the sliding distance 25 m and 82 m. Thus, the friction increased continuously from 0.6 to 1.8.

The majority of the PN coatings were removed from the pin surface between the sliding distance 25 and 82 m. Beyond 82 m sliding distance, the contact almost became 316LN/PN and the friction coefficient was steady (1.8). However, the ring coatings were not removed. It was confirmed through the 2D optical profilometer measurement on the wear track which revealed that the worn depth is considerably low ($-3.12\ \mu\text{m}$) compared to PN coating thickness ($70\ \mu\text{m}$). The SEM micrograph on the wear track which appeared as smooth surface (Fig. 8a) whereas the pin surface clearly revealed that the PN coatings were removed and then the substrate material (316LN SS) was directly contacted with the hard and rough PN surface of the ring. Therefore, the substrate material of the pin was plastically deformed and came out of the contact region (Fig. 8b). However, it produced low mean *COF* and metal loss comparatively (Figs. 9 and 10). Furthermore, the PN coating layer on the ring surface has been shown to be wear resistant whereas majority of the wear occurred on the pin surface since it contacts at a point during the sliding wear test. Thus, PN coatings have removed from the contact surface of the pin. The PN/PN Pairs produced a similar result in the air environment also [16].

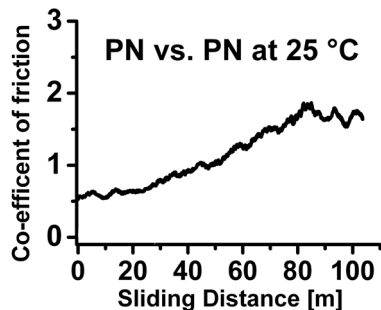


Fig. 7. The variation of *COF* as a function of sliding distance at $25\ ^\circ\text{C}$ for the PN coated ring - PN coated pin Pair

3.3 The Tribological Test on PN/PN Pair at $200\ ^\circ\text{C}$

The PN coated ring vs. PN coated pin wear test was conducted for one hour at $200\ ^\circ\text{C}$. The variation of *COF* as a function of the sliding distance is presented in Fig. 11. The friction almost remained steady from the initial state. At $200\ ^\circ\text{C}$,

the mean *COF* was the lowest (0.924) of all the tests (Fig. 9). The ring metal loss recorded was also low (Fig. 10) compared to higher temperature experiments. The SEM micrograph on the wear track was smooth with mild abrasive marks (Fig. 12a). The reason for the mild abrasive marks is that the small spherical or elliptical shape debris slide on the wear track. The wear debris collected during the experiment is shown in Fig. 12b. It contains much micron level spherical or elliptical shape debris. Therefore, the mild abrasion wear mechanism has been exhibited during this test. However, the surface damage on the ring surface is insignificant. It confirmed that PN coatings maintain its strength at lower temperature.

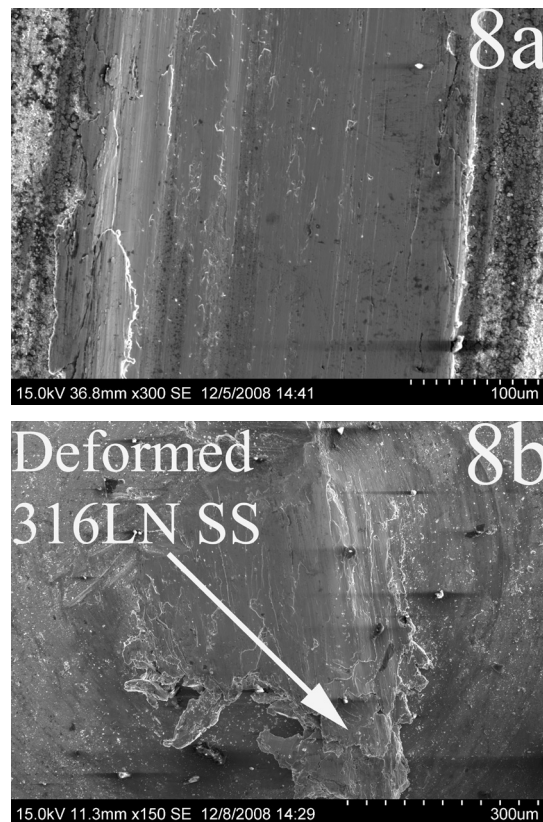


Fig. 8. SEM micrograph taken after tribological test for PN coated ring-PN coated pin Pair at $25\ ^\circ\text{C}$; a) wear track generated on PN ring; b) surface of the PN coated pin

Alternatively, there could be a possibility that friction and wear remained low at lower temperatures because of the presence of

contaminants between the contact surfaces, which could be the reason for low wear and friction at 200 °C in a vacuum environment. Similar results have been absorbed by Kazuhisa Miyoshi [8]. Therefore, PN coating eliminates the adhesion between the surfaces even in a high vacuum environment at 200 °C.

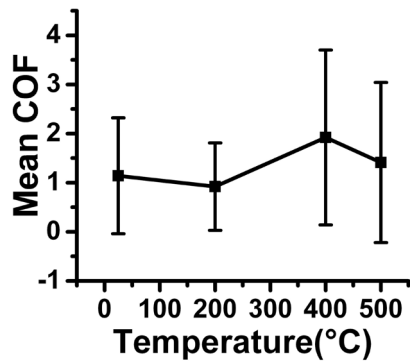


Fig. 9. The Error bar for the mean COF at 25, 200, 400 and 500 °C

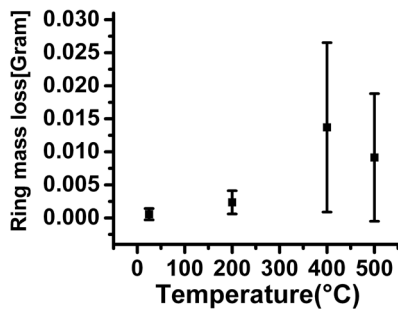


Fig. 10. The Error bar for the mass of ring metal loss at 25, 200, 400 and 500 °C

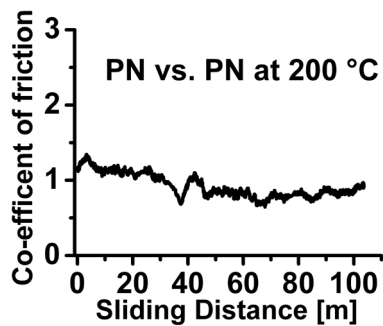


Fig. 11. The variation of COF as a function of sliding distance at 200 °C for the PN coated ring - PN coated pin Pair

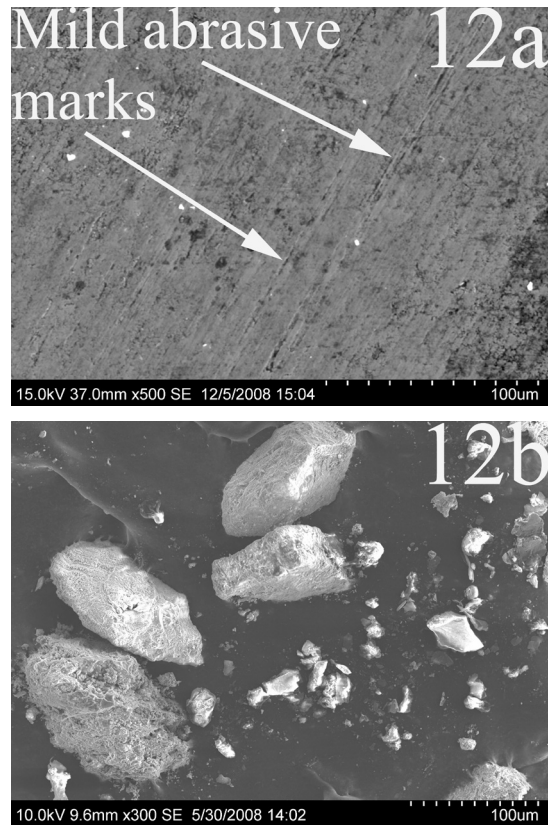


Fig. 12. SEM micrograph taken after tribological test for PN coated ring – PN coated pin Pair at 200 °C; a) wear track generated on PN ring; b) wear debris

3.4 The Tribological Test on PN/PN Pair at 400 °C

The PN coated ring – PN coated pin wear test was conducted for one hour at a speed of 0.0576 ms⁻¹, load of 4.1 N and at 400 °C temperature. The variation of COF as a function of sliding distance is presented in Fig. 13. The mean friction and ring metal loss was very high at 400 °C (Figs. 9 and 10) and the worn surface generated showed more grooves (Fig. 14a). The pin PN layer was removed from the pin contact region during the beginning stage of the experiment itself. Therefore, the pin surface plastically deformed in which the harder and sharper worn particles have embedded (Fig. 14b). At 400 °C the base metal (316LN SS) of pin was softened and held the worn particles. Then, it made grooves on the ring surface. Therefore, the wear mechanism involved was abrasive. The 2D

optical profilometer measurement on the wear track reveals that the worn depth was shallow ($-5.2 \mu\text{m}$) compared to PN layer thickness ($70 \mu\text{m}$). Therefore, PN coatings were not removed from the ring surface and PN layer on the ring surface was proved as an excellent wear resistant layer at $400 \text{ }^\circ\text{C}$ in a high vacuum environment, whereas the coatings were removed only from the pin surface since it contacts at a point during the sliding wear test.

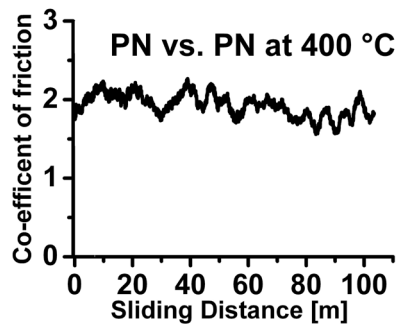


Fig. 13. The variation of COF as a function of sliding distance at $400 \text{ }^\circ\text{C}$ for the PN coated ring - PN coated pin Pair

3.5 The Tribological Test on PN/PN Pair at $500 \text{ }^\circ\text{C}$

The variation of COF as a function of the sliding distance for the tribological pair of PN vs. PN pair at $500 \text{ }^\circ\text{C}$ is presented in Fig. 15. Generally, all materials lose their hardness and mechanical properties at elevated temperatures. The CrN coatings have softened at $500 \text{ }^\circ\text{C}$ [13]. In the current work, in addition to the elevated temperature, the surfaces are atomically clean because of a high vacuum environment. Therefore, the hardness and shear strength of PN coatings as well as substrate should have reduced for both, pin and ring surfaces. Therefore, adhesion occurs between the contact surfaces. The worn surface generated at $500 \text{ }^\circ\text{C}$ had more adhesive marks which can also be seen on the surface crack (Fig. 16a). The pin coatings were immediately removed. Therefore, the substrate material (316LN SS) of the pin was plastically deformed and some worn particles embedded on the pin surface (Fig. 16b) and it made the grooves on the ring surface similar to $400 \text{ }^\circ\text{C}$. However, depth of grooves are lower

than $400 \text{ }^\circ\text{C}$. Furthermore, wear track shows the adhesive marks like pits (Fig. 16a). The weight loss scatter for 400 and $500 \text{ }^\circ\text{C}$ tests (Fig. 10) are bigger than lower temperature tests. This scatter is due to the PN layer of the removed pin with a small difference in the interval because of coating softening at elevated temperature. This is the reason why weight loss is also relatively high. In air, the PN coatings exhibit high friction and wear at lower temperatures and low at elevated temperatures [9]. Whereas in high vacuum environment, it was just reverse. Although friction and wear has decreased slightly at $500 \text{ }^\circ\text{C}$, it remained relatively higher than $200 \text{ }^\circ\text{C}$.

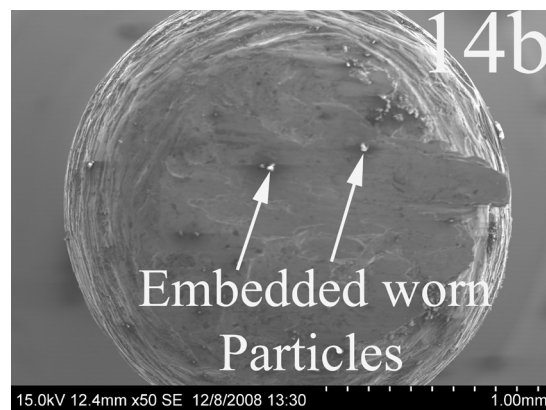
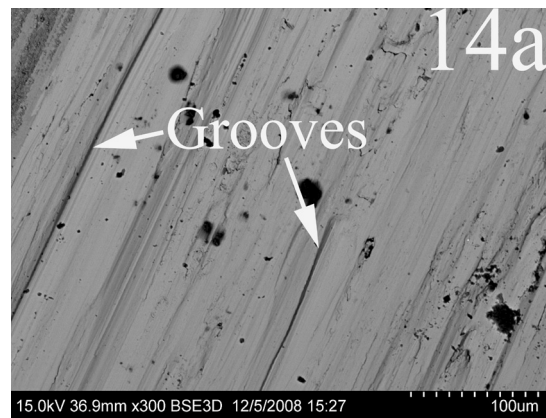


Fig. 14. SEM micrograph taken after tribological test at $400 \text{ }^\circ\text{C}$ for PN coated ring – PN coated pin Pair; a) Wear track generated on PN ring; b) surface of the PN coated pin

The PN/PN Pairs have produced low COF and low wear at lower temperatures since pin coatings were removed after the considerable

sliding distance. As long as the PN coating layer was with the pin surface, it avoids the strong adhesion between contact surfaces even in high vacuum environment and maintains lower friction and wear. At higher temperatures and a high vacuum environment, the contact surfaces are free from contaminants.

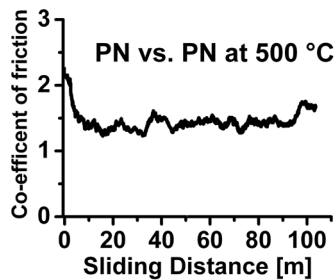


Fig. 15. The variation of COF as a function of sliding distance at 500 °C for the PN coated ring - PN coated pin Pair

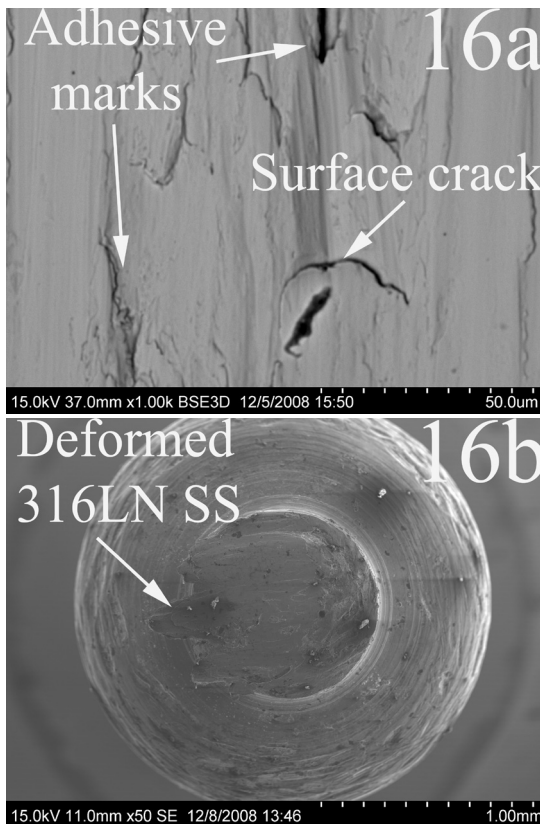


Fig.16. SEM micrograph taken after tribological test at 500 °C for PN coated ring – PN coated pin pair; a) wear track generated on PN ring; b) surface of the PN coated pin

Therefore, direct metal to metal contact occurs and it results in pin coatings being removed immediately. Thereafter, the soft pin substrate material (316LN SS) directly contacts the hard PN coating surface of the ring and exhibits very high friction and high wear. Since the pin coatings were removed in all tests, the author could not conduct the experiments for PN/PN Pairs for longer sliding distance. Hence, pin (hemispherical end) on ring configuration was not recommended to investigate the PN/PN Pairs as the pin is contacted at a point which coatings removed shortly. However, PN coatings were not removed from the ring surface whereas coating failure and subsequently plastic deformation was observed only on the pin surface. Hence, the PN coatings layer on the ring surfaces have been proved as an excellent wear resistance layer.

4 CONCLUSIONS

The COF was the highest at 400°C and lowest was at 200 °C. The friction and wear was low at lower temperatures and high at higher temperatures and it was the reverse result of air environment.

The PN layers were removed from the pin contact surface for all the PN / PN tests due to high initial contact pressure (2 GPa) and pin substrate material was plastically deformed. Hence, it is concluded that the pin (hemispherical end) on disc configuration is not recommended to investigate the wear resistance of PN/PN Pairs.

However, PN/PN Pairs maintain lower COF as long as the PN layer was attached to the pin surface since it avoids the strong adhesion between the contact surfaces. Although PN coatings exhibit very high friction at elevated temperatures in a high vacuum environment, it was proved as an excellent wear resistant layer on the ring surface.

5 REFERENCES

- [1] Smith, A.F. (1986). Influence of environment on the unlubricated wear of 316 stainless steel at room temperature. *Tribology International*, vol. 19, p. 1-10, DOI:10.1016/0301-679X(86)90088-5.

- [2] Larisch, B., Brusky, U., Spies, H.J. (1999). Plasma nitriding of stainless steels at low temperatures. *Surface and Coatings Technology*, vol. 116-119, p. 205-211, DOI: 10.1016/S0257-8972(99)00084-5.
- [3] Musil, J., Vlček, J., Růžička, M. (2000). Recent progress in plasma nitriding. *Vacuum*, vol. 59, p. 940-951, DOI:10.1016/S0042-207X(00)00404-8.
- [4] Borges, C.F.M., Hennecke, S., Pfender, E. (2000). Decreasing chromium precipitation in AISI 304 stainless steel during the plasma-nitriding process. *Surface and Coatings Technology*, vol. 123, p. 112-121, DOI:10.1016/S0257-8972(99)00506-X.
- [5] Collins, G.A., Hutchings, R., Short, K.T., Tendys, J., Li, X., Samandi, M. (1995). Nitriding of austenitic stainless steel by plasma immersion ion implantation. *Surface and Coatings Technology*, vol. 74-75, p. 417-424, DOI:10.1016/0257-8972(95)08370-7.
- [6] Hannula, S.P., Nenonen, P., Hirvonen, J.P. (1989). Surface structure and properties of ion nitride austenitic stainless steel. *Thin Solid Films*, vol. 181, p. 343-350, DOI:10.1016/0040-6090(89)90502-6.
- [7] Marchev, K., Cooper, C.V., Blucher, J.T., Giessen, B.C. (1998). Conditions for the formation of a martensite single-phase compound layer in ion-nitrided 316L austenitic stainless steel. *Surface and Coatings Technology*, vol. 99, p. 225-228, DOI:10.1016/S0257-8972(97)00532-X.
- [8] Miyoshi, K. (1999). Considerations in vacuum tribology (adhesion, friction, wear, and solid lubrication in vacuum). *Tribology International*, vol. 32, p. 605-616. DOI:10.1016/S0301-679X(99)00093-6.
- [9] Buckley, D.H. (1981). *Surface effects in adhesion, friction, wear and lubrication*. Elsevier Scientific Publishing Company, New York.
- [10] Karamis, M.B., Gercekcioglu, E. (2000). Wear behaviour of plasma nitride steels at ambient and elevated temperatures. *Wear*, vol. 243, p. 76-84, DOI:10.1016/S0043-1648(00)00426-9.
- [11] Taktak, S., Ulker, S., Gunes, I. (2008). High temperature wear and friction properties of duplex surface treated bearing steels. *Surface and Coatings Technology*, vol. 202, p. 3367-3377.
- [12] Staia, M.H., PérezDelgado, Y., Sanchez, C., Castro, A., Bourhis, E.Le., Puchi-Cabrera, E.S. (2009). Hardness properties and high-temperature wear behavior of nitrided AISI D2 tool steel, prior and after PAPVD coating. *Wear*, vol. 267, p. 1452-1461, DOI:10.1016/j.wear.2009.03.045.
- [13] Polcar, T., Parreira, N.M.G., Novák, R. (2007). Friction and wear behaviour of CrN coating at temperatures up to 500 °C. *Surface and Coatings Technology*, vol. 201, p. 5228-5235, DOI:10.1016/j.surfcoat.2006.07.121.
- [14] Bhaduri, A.K., Indira, R., Albert, S.K., Rao, B.P.S., Jain, S.C., Asokkumar, S. (2004). Selection of hardfacing material for components of the Indian Prototype Fast Breeder Reactor. *Journal of Nuclear Material*, vol. 334, p. 109-114, DOI:10.1016/j.jnucmat.2004.05.005.
- [15] Konca, E., Cheng, Y.T., Weiner, A.M., Dasch, J.M., Alpas, A.T. (2005). Vacuum tribological behavior of the non-hydrogenated diamond-like carbon coatings against aluminum: Effect of running-in in ambient air. *Wear*, vol. 259, p. 795-799, DOI:10.1016/j.wear.2005.02.034.
- [16] Devaraju, A., Elayaperumal, A. (2010). Tribological behaviors of plasma nitrided AISI 316 LN type stainless steel in air and high vacuum atmosphere at room temperature. *International Journal of Engineering Science and Technology*, vol. 2, no. 9, p. 4137-4146.